Journal of Structural Biology 184 (2013) 33–42

Contents lists available at SciVerse ScienceDirect

Journal of Structural Biology

journal homepage: www.elsevier.com/locate/yjsbi

Structure of the ParM filament at 8.5 Å resolution

Pananghat Gayathri [a,2], Takashi Fujii [b,1,2], Keiichi Namba [b,c], Jan Löwe [a,*]

[a] MRC Laboratory of Molecular Biology, Hills Road, Cambridge CB2 0QH, UK
[b] Graduate School of Frontier Biosciences, Osaka University, 1-3 Yamadaoka, Suita, Osaka 565-0871, Japan
[c] Riken Quantitative Biology Centre, 1-3 Yamadaoka, Suita, Osaka 565-0871, Japan

ARTICLE INFO

Article history:
Available online 24 February 2013

Keywords:
Bacterial cytoskeleton
Actin
Cytomotive
Dynamic instability

ABSTRACT

The actin-like protein ParM forms the cytomotive filament of the ParMRC system, a type II plasmid segregation system encoded by *Escherichia coli* R1 plasmid. We report an 8.5 Å resolution reconstruction of the ParM filament, obtained using cryo-electron microscopy. Fitting of the 3D density reconstruction with monomeric crystal structures of ParM provides insights into dynamic instability of ParM filaments. The structural analysis suggests that a ParM conformation, corresponding to a metastable state, is held within the filament by intrafilament contacts. This filament conformation of ParM can be attained only from the ATP-bound state, and induces a change in conformation of the bound nucleotide. The structural analysis also provides a rationale for the observed stimulation of hydrolysis upon polymerisation into the filament.

1. Introduction

ParMRC, the eponymous Type II plasmid segregation system, provides a well-documented example of an actin-like double helical filament functioning as a linear motor, by actively pushing R1 plasmids towards the cell poles of *Escherichia coli* (Gerdes et al., 2010; Salje et al., 2010). Hence filaments of the ParM protein have been classified as cytomotive (Löwe and Amos, 2009). The system comprises three components: ParM, a polymerising motor of actin fold, *parC*, a centromeric, repeated DNA sequence on the plasmid and ParR, the adaptor protein that links the filament and *parC* DNA (Fig. 1). The mechanism of action of ParMRC, one of the simplest mitotic spindles, has been studied using a combination of techniques involving biochemical and immunofluorescence techniques (Møller-Jensen et al., 2003), X-ray crystallography (van den Ent et al., 2002; Møller-Jensen et al., 2007; Schumacher et al., 2007), fluorescence microscopy both *in vitro* and *in vivo* (Garner et al., 2004, 2007; Campbell and Mullins, 2007), electron microscopy (Orlova et al., 2007; Popp et al., 2008; Galkin et al., 2009), and cryo-electron microscopy of vitreous sections (CEMOVIS) of *E. coli* cells expressing ParM (Salje et al., 2009). These approaches have provided detailed mechanistic insights into the plasmid partitioning mechanism by ParMRC [reviews (Gerdes et al., 2010; Salje et al., 2010)] Fig. 1.

ParM forms actin-like double helical filaments comprising two protofilaments. In contrast to actin filaments with a right-handed twist, ParM filaments are left-handed (Orlova et al., 2007; Popp et al., 2008). They also differ from actin in their dynamic behaviour. ParM filaments exhibit dynamic instability, as opposed to the treadmilling properties of actin (Garner et al., 2004), which is thought to be an essential feature facilitating plasmid partitioning. Structural description at atomic resolution, of the various conformational states of the filament and monomeric forms of ParM is necessary for providing a molecular explanation for dynamic instability.

One of the bottlenecks for studying the structure of cytoskeletal proteins that form dynamic filaments using X-ray crystallography is that often heterogeneity due to polymerisation precludes crystallisation. Although there have been instances of protofilaments being observed in the crystal packing (van den Ent et al., 2001; Oliva et al., 2004; Aylett et al., 2010; Matsui et al., 2012), the possibility of obtaining a relevant protofilament structure is rare, especially when the filament is helical with a large repeat distance, as is the case for ParM. Hence, a hybrid approach including helical reconstruction of the filaments using cryo-electron microscopy and subsequent fitting of monomeric crystal structures into the reconstruction is suitable for studying the structures of dynamic cytoskeletal protein filaments. In recent years, technical advances in cryo-electron microscopy have resulted in sub-nanometre resolution reconstructions of filaments (Egelman, 2007; Fujii et al., 2009). Successful examples include actin filaments (Fujii et al., 2010), flagellar polyhooks (Fujii et al., 2009) and needle filaments of the Type III secretion system (Fujii et al., 2012).

* Corresponding author. Fax: +44 1223 213556.
E-mail addresses: jyl@mrc-lmb.cam.ac.uk, jan.d.k.lowe@gmail.com (J. Löwe).
[1] Present address: Riken Quantitative Biology Centre, 1-3 Yamadaoka, Suita, Osaka 565-0871, Japan.
[2] PG and TF contributed equally to this work.

1047-8477/$ - see front matter © 2013 Elsevier Inc. All rights reserved.
http://dx.doi.org/10.1016/j.jsb.2013.02.010

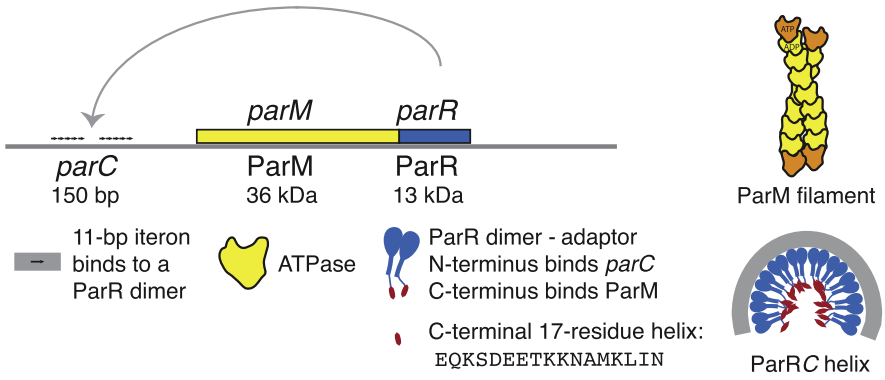

Fig. 1. Schematic representation of the components of the ParMRC system. The operon for the ParMRC system consists of ParM and ParR regulated by the centromeric region of *parC*. ParM is an ATPase of actin fold, and forms double helical filaments. ParR is a repressor of ParM and ParR expression and also the adaptor between the DNA and the filaments. It links the *parC* DNA and the end of ParM filaments. Ten ParR dimers bind to the ten iterons (11-base pairs each) of *parC* and form the ParRC helical ring.

In this work, we describe an 8.5 Å cryo-electron microscopy reconstruction of the ParM filament. Previous electron microscopy reconstructions of the ParM filament provided much lower resolution pictures (Orlova et al., 2007; Popp et al., 2008; Galkin et al., 2009). The low resolution of the reconstructions has previously led to many debates about the filament structure, even including the polarity of the protofilaments (Erickson, 2012; Galkin et al., 2012). The subnanometer resolution of the current reconstruction confirms the double-helical, polar structure of ParM filaments. Based on the comparison of the reconstruction with crystal structures of ParM in the monomeric states, we discuss how monomer and nucleotide conformations in the filament state contribute to the dynamic instability of ParM filaments. In addition to the cryo-EM reconstruction, the current analysis includes crystal structures of four different conformational states of ParM, thus complementing the existing information about dynamic instability of ParM (Popp et al., 2008; Galkin et al., 2009). These insights are relevant not only to the plasmid partitioning mechanism by ParM, but also relate to questions in other dynamic filament systems such as other bacterial actin-like proteins, F-actin and even microtubules in the eukaryotic cytoskeleton.

The sub-nanometer resolution reconstruction also led to elucidation of the mechanism for plasmid partitioning. Based on the structural data and TIRF (total internal reflection fluorescence) microscopy studies, it was shown that ParRC binds to only one end of ParM filaments, and a bipolar spindle of antiparallel ParM filaments drives plasmid segregation (Gayathri et al., 2012). The present work describes a detailed structural analysis of the structures reported in (Gayathri et al., 2012) that leads to a mechanistic explanation for dynamic instability of ParM filaments.

2. Materials and methods

2.1. Cryo-electron microscopy reconstruction of ParM filaments

A high-resolution cryoEM reconstruction of the ParM filament (Fig. 2A and B) was obtained as previously reported (Gayathri et al., 2012). Briefly, ParM filaments were prepared by incubating 30 μM ParM protein in 200 μl polymerisation buffer (30 mM Tris–HCl, 25 mM KCl, 2 mM $MgCl_2$, 1 mM DTT, pH 7.5) with 5 mM AMP-PNP for 5 min at room temperature. The filaments were spun down to remove monomers and resuspended in 40 μl buffer. A 2.1 μl sample solution was applied onto a Quantifoil holey carbon molybdenum grid (R0.6/1.0, Quantifoil Micro Tools GmbH, Jena, Germany) and was plunge-frozen into liquid ethane using a vitrification device (Vitrobot, FEI). The specimen was observed at temperatures of 50–60 K using a JEOL JEM3200FSC electron microscope, equipped with an Ω-type energy filter and operated at 200 kV. Zero energy-loss images, with a slit setting to remove electrons of an energy-loss larger than 10 eV, were recorded on a 4 k × 4 k 15 μM/pixel slow-scan CCD camera, TemCam-F415MP (TVIPS, Germany) at a magnification of 91,463, a defocus range of 0.7–2.0 μM and an electron dose of ~20 electrons/$Å^2$. The magnification was calibrated by the layer line spacing of 23.0 Å of tobacco mosaic virus mixed in the sample solution. The image pixel size at this magnification was 1.64 Å/pixel. 200 CCD images were collected.

Defocus and astigmatism in the images were determined using CTFFIND3 (Mindell and Grigorieff, 2003). Images of the ParM filament were boxed into 20,917 segments of 512 × 512 pixels with a step shift of 100 pixels along the helical axis using EMAN's boxer program (Ludtke et al., 1999). Images were then phase-corrected by multiplying a phase and amplitude contrast transfer function (CTF) with the astigmatism obtained by CTFFIND3. We used a ratio of 7% for the amplitude CTF to the phase CTF. This procedure results in the multiplication of the square of the CTF (CTF^2) to the original structure factor and suppresses the noise around the nodes of the CTF, allowing more accurate image alignment. This amplitude modification was corrected in the last stage of image analysis. The images were then high-pass filtered (285 Å), normalised and cropped to 320 × 320 pixels. Image processing was mainly carried out with the SPIDER package (Frank et al., 1996) on a PC cluster computer (RC server Calm2000, Real Computing, Tokyo, Japan).

Projection images were generated from each reference volume at every 1° rotation about the filament axis from 0 to 360° to produce all views. The raw images of the boxed ParM segments were aligned and cross-correlated with the set of reference projections to produce the following information: an in-plane rotation angle, an *x*-shift, a *y*-shift, an azimuthal angle and a cross-correlation coefficient for each segment. Image segments with a small cross-correlation coefficient were discarded. The polarity was tracked and the orientation was determined from the majority for each filament. Image segments identified to have the opposite orientation were discarded. On average, 95% of the segments from each filament showed the same polarity. A 3D reconstruction was then generated by back-projection. The symmetry of this new volume was determined by a least-squares fitting algorithm and was imposed upon the reconstruction (Egelman, 2000). The new volume was used as a reference for the next round of alignment. This process was repeated iteratively until the symmetry values converged. The initial parameters were 24.7 Å for axial rise and 163° for azimuthal rotation along the 1-start helix, and they were converged to 23.62 Å and 164.98°, respectively. The Fourier transform of the reconstruction was then multiplied by $1/[CTF^2 + 1/SNR]$ to correct for the amplitude distortion by the CTF. The map was sharpened with a B-factor of −200 $Å^2$. The statistics of the EM reconstruction is tabulated in (Gayathri et al., 2012).